AD-A070 112 ROME AIR DEVELOPMENT CENTER GRIFFISS AFB NY F/G 9/5
A STUDY OF THE SCANNING PROPERTIES OF SOME SIMPLE REFLECTIONS,(U)
FEB 79 R L FANTE, K M ROMBERG
UNCLASSIFIED RADC-TR-79-34 NL

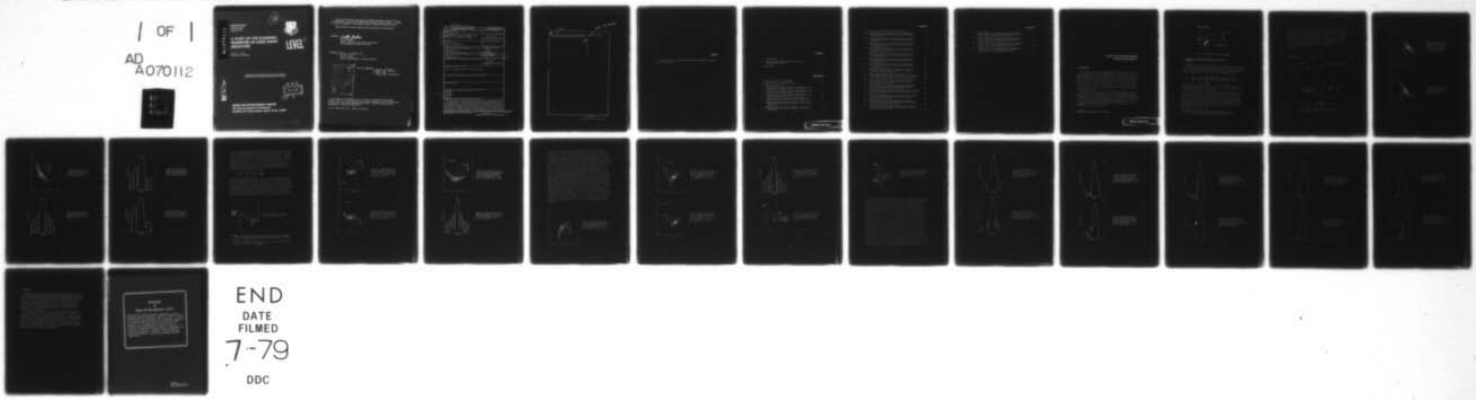

END
DATE FILMED
7-79
DDC

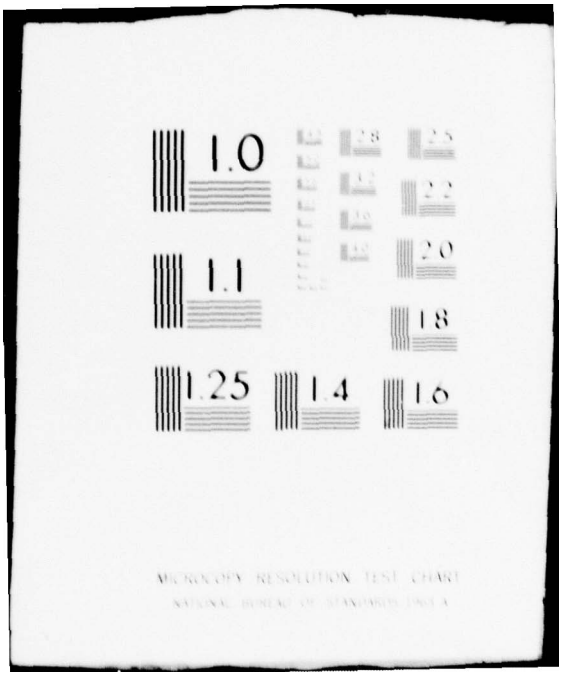
1.0
1.1
1.25
1.4
1.6
2.8
2.5
2.2
2.0
1.8
MICROCOPY RESOLUTION TEST CHART
NATIONAL BUREAU OF STANDARDS 1963 A

RADC-TR-79-34
In-House Report
February 1979

A STUDY OF THE SCANNING PROPERTIES OF SOME SIMPLE REFLECTORS

Ronald L. Fante
Katherine M. Romberg

LEVEL II

ROME AIR DEVELOPMENT CENTER
Air Force Systems Command
Griffiss Air Force Base, New York 13441

This report has been reviewed by the RADC Information Office (OI) and is releasable to the National Technical Information Service (NTIS) At NTIS it will be releasable to the general public, including foreign nations.

RADC-TR-79-34 has been reviewed and is approved for publication.

APPROVED: Walter Rotman

WALTER ROTMAN
Chief, Antennas and RF Components Branch
Electromagnetic Sciences Division

APPROVED: Allan C. Schell

ALLAN C. SCHELL
Chief, Electromagnetic Sciences Division

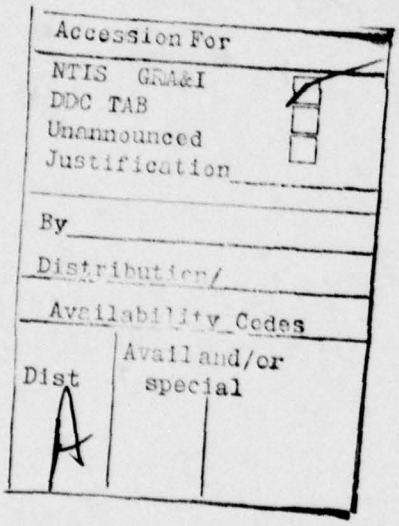

FOR THE COMMANDER: John P. Huss

JOHN P. HUSS
Acting Chief, Plans Office

If your address has changed or if you wish to be removed from the RADC mailing list, or if the addressee is no longer employed by your organization, please notify RADC (EEA) Hanscom AFB MA 01731. This will assist us in maintaining a current mailing list.

Do not return this copy. Retain or destroy.

Unclassified

SECURITY CLASSIFICATION OF THIS PAGE (When Data Entered)

REPORT DOCUMENTATION PAGE	READ INSTRUCTIONS BEFORE COMPLETING FORM
1. REPORT NUMBER: RADC-TR-79-34 / 2. GOVT ACCESSION NO.	3. RECIPIENT'S CATALOG NUMBER
4. TITLE (and Subtitle): A STUDY OF THE SCANNING PROPERTIES OF SOME SIMPLE REFLECTORS	5. TYPE OF REPORT & PERIOD COVERED: In-House Report
	6. PERFORMING ORG. REPORT NUMBER
7. AUTHOR(s): Ronald L. Fante, Katherine M. Romberg	8. CONTRACT OR GRANT NUMBER(s): 2305 J3 1
9. PERFORMING ORGANIZATION NAME AND ADDRESS: Deputy for Electronic Technology (RADC/EEA), Hanscom AFB, Massachusetts 01731	10. PROGRAM ELEMENT, PROJECT, TASK AREA & WORK UNIT NUMBERS: 61102F, 2305J303
11. CONTROLLING OFFICE NAME AND ADDRESS: Deputy for Electronic Technology (RADC/EEA), Hanscom AFB, Massachusetts 01731	12. REPORT DATE: February 1979
	13. NUMBER OF PAGES: 27
14. MONITORING AGENCY NAME & ADDRESS (if different from Controlling Office)	15. SECURITY CLASS. (of this report): Unclassified
	15a. DECLASSIFICATION/DOWNGRADING SCHEDULE

16. DISTRIBUTION STATEMENT (of this Report)

Approved for public release; distribution unlimited.

17. DISTRIBUTION STATEMENT (of the abstract entered in Block 20, if different from Report)

18. SUPPLEMENTARY NOTES

19. KEY WORDS (Continue on reverse side if necessary and identify by block number)

Antennas
Radiation
Reflectors
Scanning

20. ABSTRACT (Continue on reverse side if necessary and identify by block number)

A study has been made of the scanning properties of some singly-curved reflecting surfaces. First considered was the focal region field distribution when a plane wave is incident at various angles upon the reflecting surface. The information gained from this analysis was then used to study the scanning properties of the reflectors when sources are placed in the focal region. In particular, the parabolic cylinder was first analyzed, and it was found that this surface could be scanned only several beamwidths without severe coma lobes occurring in the radiation pattern. A modified surface was then studied and

over

DD FORM 1 JAN 73 1473 EDITION OF 1 NOV 65 IS OBSOLETE

Unclassified

SECURITY CLASSIFICATION OF THIS PAGE (When Data Entered)

309 050

JOB

20. (Cont)

it was found that this surface could be scanned over ± 10 beamwidths, simply by switching the location of the feed.

Preface

We are grateful to Dr. Peter Franchi for numerous discussions and suggestions on this program.

Contents

Illustrations

A Study of the Scanning Properties of Some Simple Reflectors

1. INTRODUCTION

In this report we present some preliminary results on our attempts to develop a reflector antenna with limited scanning capabilities. The goal is to develop a reflector surface which is such that the position of the main beam of the radiation pattern can be changed simply by switching (electronically) the location of the feed which is excited. For example, exciting feed No. 1 in Figure 1 would place the main beam at $\phi = \phi_1$, exciting horn 2 would place the main beam at $\phi = \phi_2$, and so on. We will show here that it is relatively easy to develop singly curved surfaces which can be scanned over ± 10 beamwidths simply by switching the location of the feed horn which is excited.

The analysis will be performed by first considering the properties of the reflecting surface as a receiving antenna. That is, we will illuminate the reflector by a plane wave incident at $\phi = \phi_1$ and then study (using the physical optics approximation) the location and structure of the focal spot. This tells us where to place the feed, and gives us an idea of the amount of beam distortion we may expect. Once the appropriate feed location is known we then study the Fraunhofer zone field patterns produced by a feed at this point.

(Received for publication 12 February 1979)

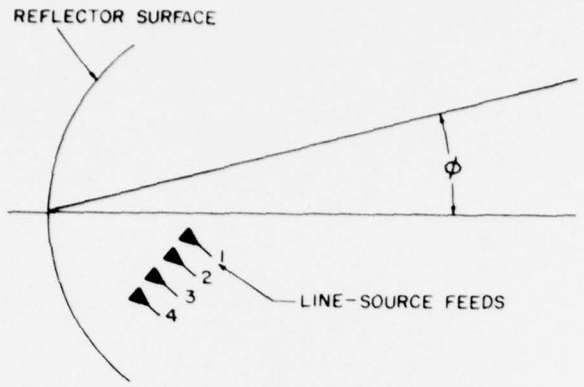

Figure 1. Example of Limited - Scan Reflector

2. RECEIVING AND TRANSMITTING PATTERNS OF A REFLECTING SURFACE

Consider the single-curved reflecting surface* in Figure 2, which is illuminated by a plane wave with magnetic field given by $\underline{H}_i = (\hat{x} \cos\phi + \hat{z} \sin\phi) \exp(-ikz \cos\phi + ik x \sin\phi)$. Then the magnetic field at the point (x, z) due to the diffraction of the incident magnetic field is given by the physical optics approximation as[1]

$$\underline{H}(x, z) = \left(\frac{ik}{2\pi}\right)^{1/2} \int_A \frac{dx \left\{\left(\hat{z} - \hat{x}\frac{\partial f}{\partial x}\right) \times \underline{H}_i\right\} \times \left\{(x'-x)\,\hat{x} + (z'-z)\,\hat{z}\right\}}{\rho^{3/2}} \cdot \exp(-ik\rho) \qquad (1)$$

where $k = 2\pi/\lambda$, λ = signal wavelength, $\rho = \left[(x'-x)^2 + (z'-z)^2\right]^{1/2}$, A is the projection of the reflector surface onto the x axis, $z = f(x)$ is the equation satisfied by the reflecting surface and $\hat{x}$, $\hat{z}$ are unit vectors.

Equation (1) has been used to compute the magnetic field distribution as a function of angle of incidence for an offset parabolic cylinder, as shown in Figure 3. Contour plots of the magnetic field amplitude are shown in Figures 4 to 6. Note that when $\phi = 0°$ there is a well-defined focal spot, but as the angle of incidence is increased the spot becomes deformed and elongated. The bending of the contours in Figure 6 follows the caustic surfaces. The same conclusion holds for the non-offset parabola; a well-defined spot is produced for $\phi = 0°$, but the spot becomes highly distorted as ϕ is increased.

---

*The reflector is assumed to be of infinite extent in the y - direction.

1. Silver, S. (1965) Microwave Antenna Theory and Design, Dover, N. Y.

We have also considered the inverse problem in which line sources are alternately placed at the center of the focal spots in Figures 4 to 6 and the corresponding radiation pattern of the parabolic cylinder then calculated. Results for the case when the line source feed is isotropic are shown in Figures 7 to 9. As expected, the pattern is symmetric when the main beam is centered at $\phi = 0°$, but is highly assymmetric (coma) when the feed is placed such that the main beam is centered at $\phi = 10°$. Therefore, the parabolic cylinder, or offset parabolic cylinder has poor scanning properties and is not the most useful surface for a limited-scan reflector.

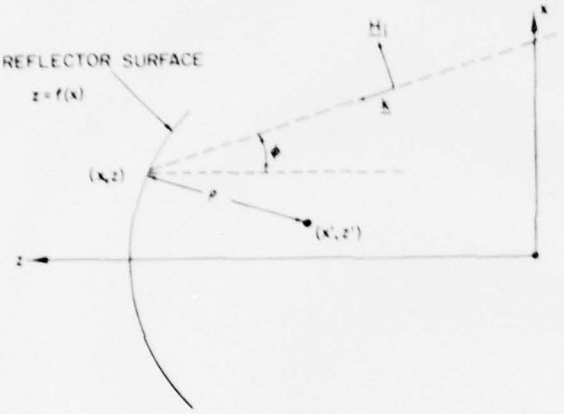

Figure 2. Reflector Treated as a Receiving Antenna

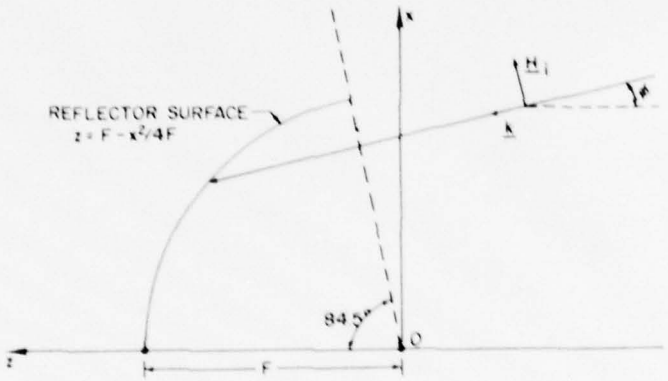

Figure 3. Offset Parabolic Cylinder. The ratio of the focal length, F, to diameter, D, is F/D = 1/2

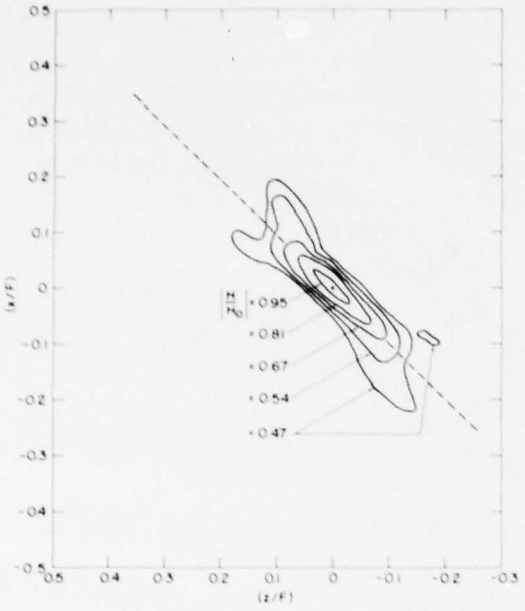

Figure 4. Contour Plot of the Received Magnetic Field Amplitude for the Reflector Shown in Figure 3, for $F = 15\lambda$ and $\phi = 0°$. H_o is the magnetic field amplitude at the center of the spot

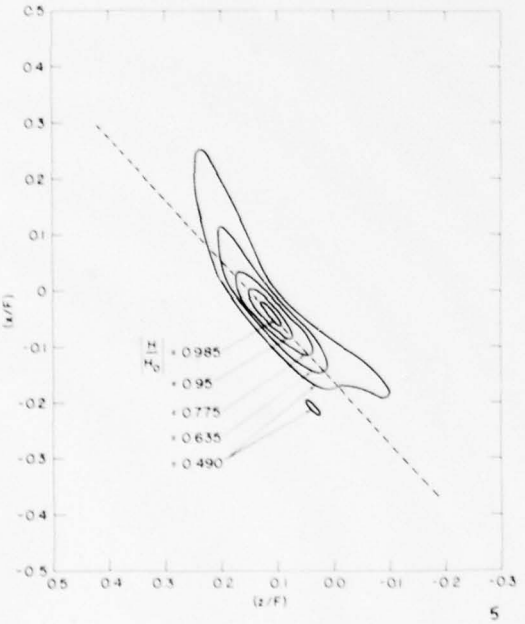

Figure 5. Contour Plot of the Received Magnetic Field Amplitude for the Reflector Shown in Figure 3, for $F = 15\lambda$ and $\phi = 5°$

5

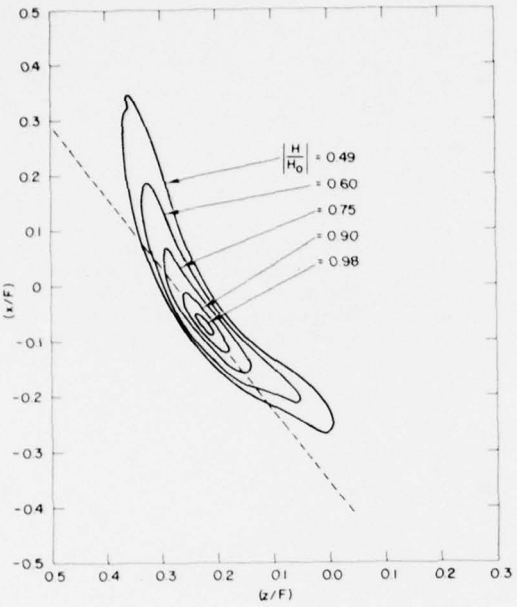

Figure 6. Contour Plot of the Received Magnetic Field Amplitude for the Reflector Shown in Figure 3, for $F = 15\lambda$ and $\phi = 10^\circ$

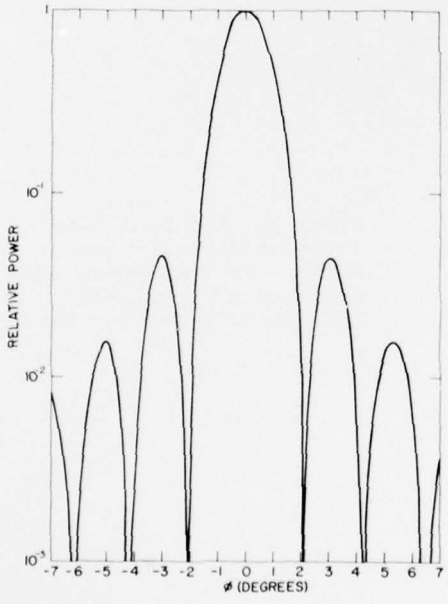

Figure 7. Radiation Pattern of the Parabolic Cylinder in Figure 3 for an Isotropic Line Source at $x/F = 0$, $z/F = 0$, With $F = 15\lambda$

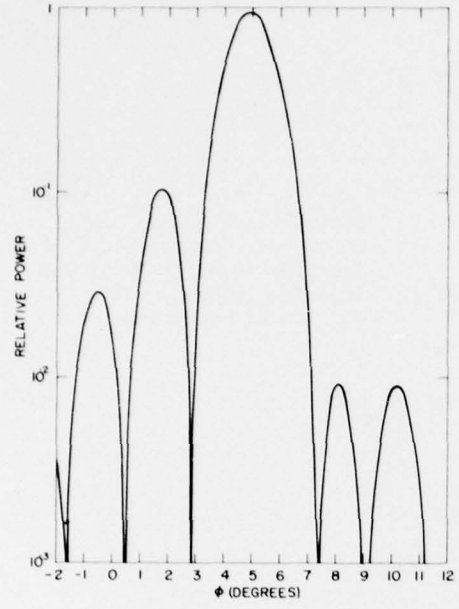

Figure 8. Radiation Pattern of the Parabolic Cylinder in Figure 3 for an Isotropic Line Source at x/F = -0.03833, z/F = 0.1117, With F = 15λ

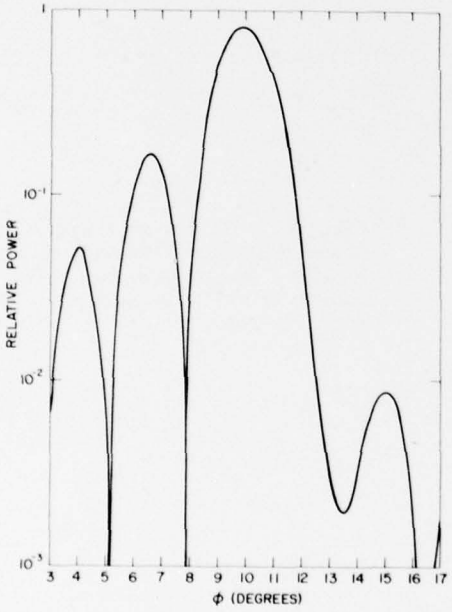

Figure 9. Radiation Pattern of the Parabolic Cylinder in Figure 3 for an Isotropic Line Source at x/F = -0.0633, z/F = 0.2267, With F = 15λ

The difficulty with the parabola is that it is perfectly focused for $\phi = 0°$, but becomes rapidly defocused when one scans to other values of ϕ. On the other hand a circular cylinder has the disadvantage of being poorly focused for $\phi = 0°$ but this system does not deteriorate rapidly as one scans to other values of ϕ. It would be desirable to find a surface which is not as well focused as the parabolic cylinder nor as poorly focused as the circular cylinder, but which has better scanning properties than the parabolic cylinder. One surface which has this property is a modification of a scan corrected surface[2,3] developed for another purpose. The surface we have studied satisfies the equation

$$r = r_o \left[1 + \frac{\theta^2}{3} + \frac{3}{45}\theta^4 + \frac{2}{135}\theta^6 + \frac{\theta^8}{2025} \right] \tag{2}$$

where r and θ are shown in Figure 10. We first studied the properties of this surface when used as a receiving antenna. The results for the case when the surface is symmetric about the z-axis (with $\theta_0 = -45°$ and $\theta_1 = 45°$) are shown in Figures 11 to 13. Note that there is a well-focused spot for the angle of incidence, ϕ, equal to 0° but that the spot becomes defocused as ϕ is increased. The radiation pattern produced when an isotropic line source, placed at the center of the focal spot in Figure 11, illuminates the reflector is shown in Figure 14. Note that the sidelobe levels are about 3 dB lower than those for the corresponding circular cylinder.[4]

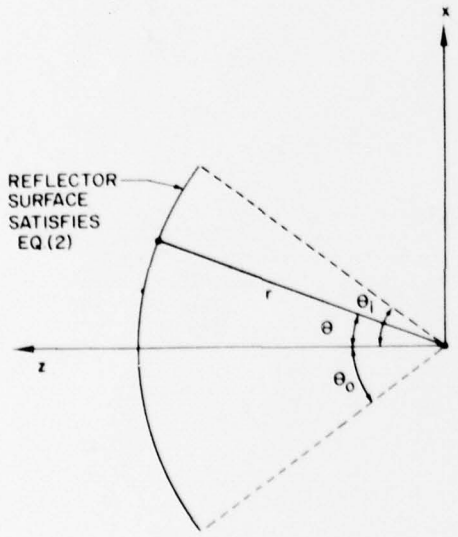

Figure 10. Geometry for Study of the Surface Defined by Eq. (2)

2. Schell, A. (1973) Performance of a Reflector-Array Limited Scan Technique, Digest of IEEE Antennas & Propagation Symposium, Boulder, CO, pp 318-320.

3. McGahan, R. (private communication).

4. Holt, F., and Bouche, E. (1964) A Gregorian corrector for spherical reflectors, IEEE Trans. on Ant. & Prop. AP-12:44-47.

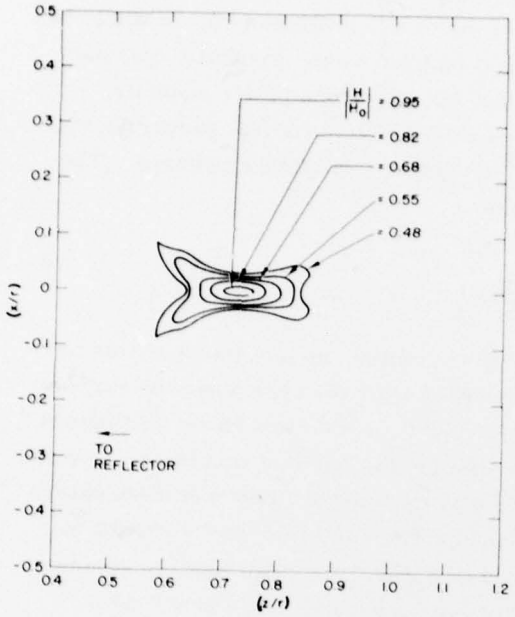

Figure 11. Contour Plot of the Received Magnetic Field Amplitude When the Reflector Defined by Eq. (2) is Illuminated by a Plane Wave at $\phi = 0°$. Also, $\theta_o = -45°$, $\theta_1 = 45°$, and $r_o = 15\lambda$

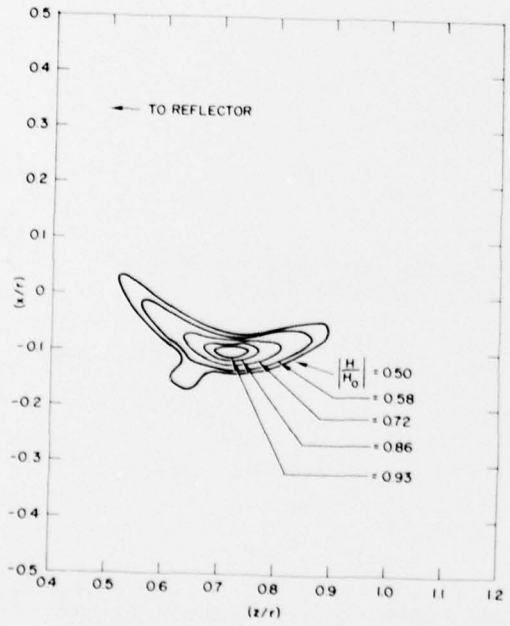

Figure 12. Contour Plot of the Received Magnetic Field Amplitude When the Reflector Defined by Eq. (2) is Illuminated by a Plane Wave at $\phi = 7°$. Also, $\theta_o = -45°$, $\theta_1 = 45°$, and $r_o = 15\lambda$

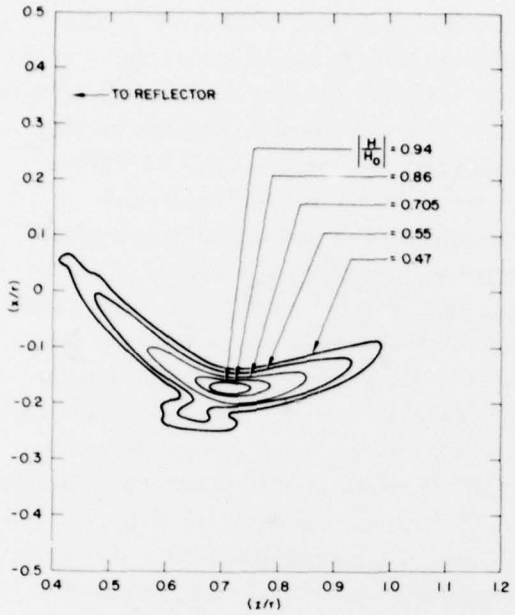

Figure 13. Contour Plot of the Received Magnetic Field Amplitude When the Reflector Defined by Eq. (2) is Illuminated by a Plane Wave Incident at $\phi = 12°$. Also, $\theta_o = -45°$, $\theta_1 = 45°$, and $r_o = 15\lambda$

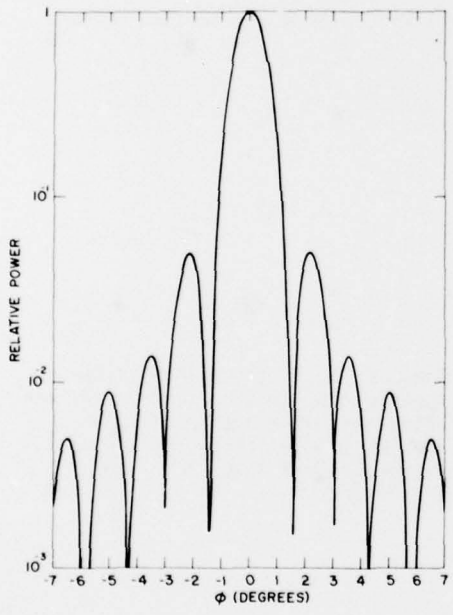

Figure 14. Radiation Pattern of the Reflector Defined by Eq. (2) for an Isotropic Line Source at $x/r_o = 0.0$, $z/r_o = 0.277$, With $r_o = 25\lambda$, $\theta_o = 45°$, and $\theta_1 = 45°$

Next let us consider the receiving properties of an asymmetric surface [satisfying Eq. (2)] with edges at the angles $\theta_o = -80.5°$ and $\theta_1 = 0°$. In this case, as is evident from Figures 15 to 17, the spot is well focused when the angle, ϕ, of incidence of the plane wave is equal to 12° but poorly focused when $\phi = 0°$. The corresponding radiation pattern when an isotropic field is placed at the center of the focal spot in Figure 17 is shown in Figure 18. Observe the excellent pattern. Therefore, different portions of the surface in Eq. (2) focus differently, with the portion near $\theta = 0°$ producing a well-behaved radiation pattern centered at $\theta = 0°$ and the portion near $\theta = -45°$ producing a well-behaved radiation pattern centered at $\phi = 12°$. Consequently, we shall study the capabilities of this surface for limited scanning. In particular, we shall consider the situation shown in Figure 19. The reflector surface occupies the entire angular region from $\theta = -\pi/2$, to $\theta = \pi/2$, and directive line sources are placed along the arc which defines the locus of the well-focused spots (as determined from Figures 11 to 13, Figure 15 to 17, and similar results, when portions of the reflector are used as a receiving antenna). Each line source is centered on a different point of the reflector and illuminates a different (although overlapping) portion of the reflector, as shown in Figure 20. For example, from Figure 17 it is clear that if we want to produce a beam centered at $\phi = 12°$ we should excite a source at $x/r_o = -0.154$, $z/r_o = 0.2$ which illuminates (between its 3 dB points) roughly the angular region from $\theta = -80.5°$ to $\theta = 0°$, and has low sidelobes outside this range of angles. Similarly, in order to produce a beam centered on $\phi = 0°$ we would excite a source at $x = 0$, $z/r_o = 0.277$ which illuminates roughly the angular region from $\theta = -45°$ to $\theta = 45°$, with low sidelobes outside this region.

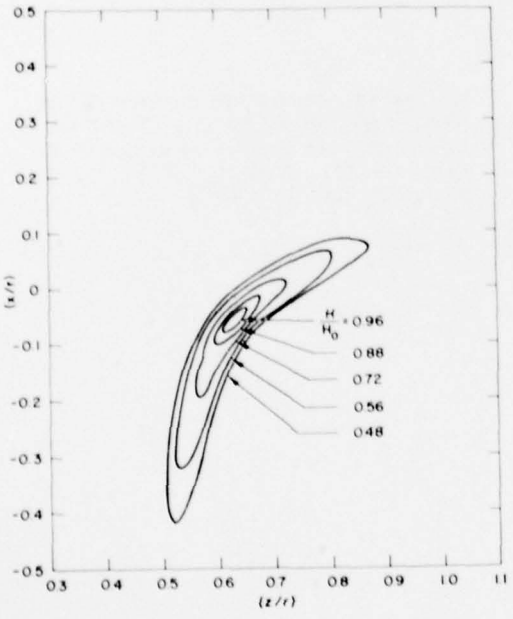

Figure 15. Contour Plot of the Received Magnetic Field Amplitude When the Reflector Defined by Eq. (2) is Illuminated by a Plane Wave Incident at $\phi = 0°$. Also, $\theta_o = -80.5$, $\theta_1 = 0°$ and $r_o = 15\lambda$

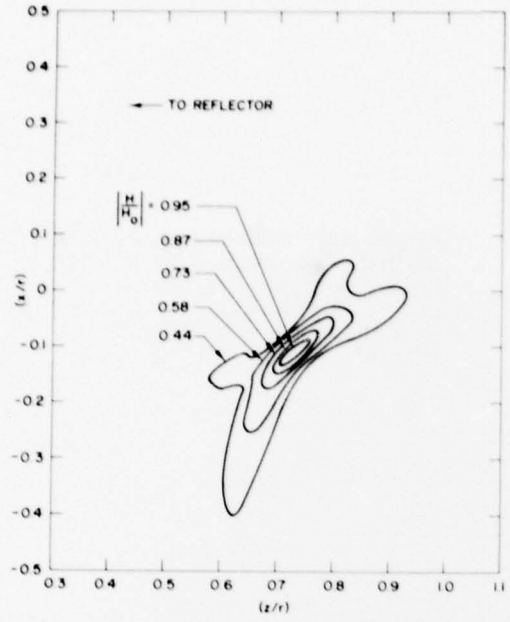

Figure 16. Contour Plot of the Received Magnetic Field Amplitude When the Reflector Defined by Eq. (2) is Illuminated by a Plane Wave Incident at $\phi = 7°$. Also, $\theta_o = -80.5°$, $\theta_1 = 0°$ and $r_o = 15\lambda$

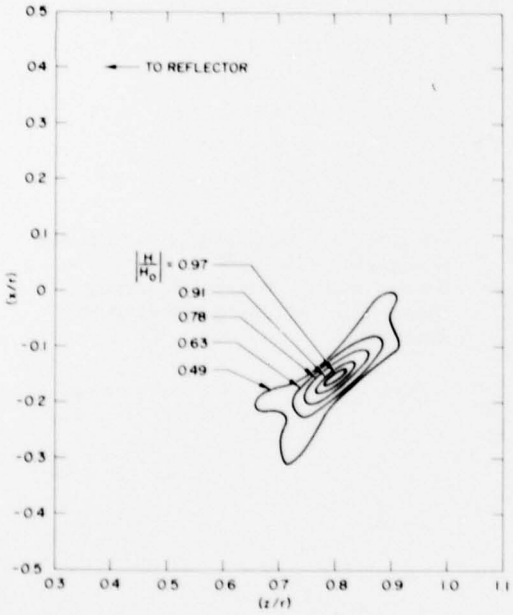

Figure 17. Contour Plot of the Received Magnetic Field Amplitude When the Reflector Defined by Eq. (2) is Illuminated by a Plane Wave Incident $\phi = 12°$. Also, $\theta_o = -80.5°$, $\theta_1 = 0°$ and $r_o = 15\lambda$

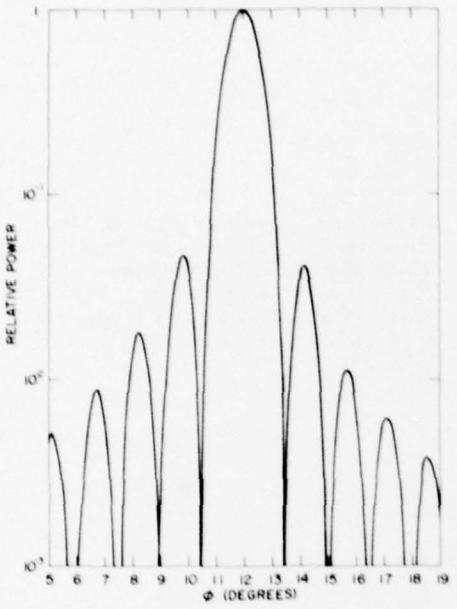

Figure 18. Radiation Pattern of the Reflector Defined by Eq. (2) for an Isotropic Line Source at $x/r_o = -0.154$, $z/r_o = 0.2$ With $r_o = 25\lambda$, $\theta_o = -80.5°$, and $\theta_1^o = 0°$

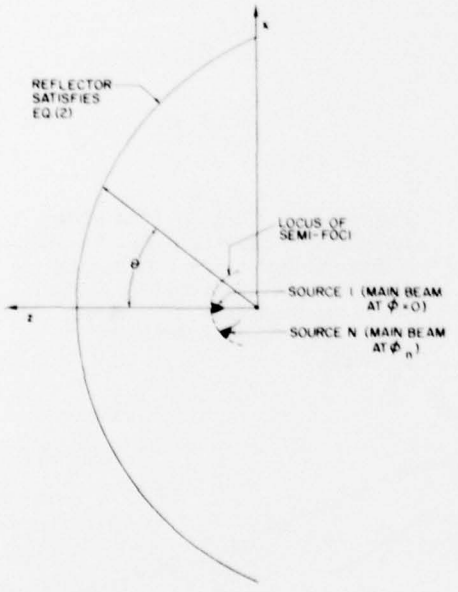

Figure 19. Method of Illuminating the Surface Defined by Eq. (2) so as to Give Electronic Scanning Simply by Switching the Source Excited

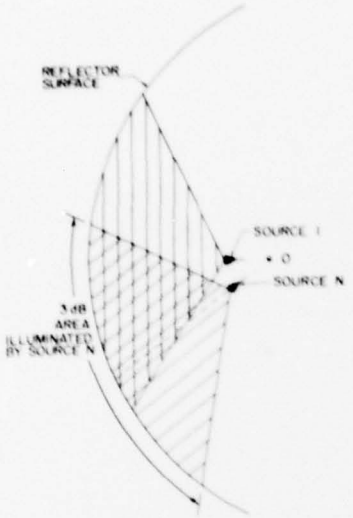

Figure 20. Area Illuminated, Between 3 dB Points, by the Nth Line Source. This source produces a radiation pattern with main beam at $\phi = \phi_N$

Some results for the scanning properties of the surface in Figure 19 are shown in Figures 21 to 25. The beam position is switched by switching the excitation from one line source to another. Each line source illuminates a sector of roughly 60° (from 3 dB to 3 dB point) and this gives an effective F/D ratio of 0.6 where F is the effective focal length and D is the diameter of the illuminated section. The sidelobe level of the illuminating radiation is roughly -13 dB. From Figures 21 to 25 we see that this system has reasonably good scanning characteristics for all angles from $-14.5° < \phi < 14.5°$ (about ± 10 beamwidths); the pattern begins to exhibit coma for $\phi \geq \pm 14.5°$. The only undesirable features of the patterns are the shoulders on the main beam in Figure 21, and the far-out sidelobes in Figures 21 to 25. These latter sidelobes can be eliminated by using a feed pattern with lower sidelobes. Therefore, if we use an illumination which has approximately the same beamwidth as before, but with -26 dB sidelobes instead of -13 dB sidelobes we obtain the reflector radiation patterns shown in Figures 26 to 30. We note that the far-out sidelobes have disappeared, but that the shoulders in the pattern in Figure 26 remain. Unfortunately, these shoulders cannot be eliminated without further reducing the antenna efficiency, because they are produced by stationary points (specular points at $\theta = \pm 40.5°$ in the phase function of the integrand of the radiation pattern integral. Consequently, unless the illumination produced by the feed horn has a notch at $\theta = \pm 40.5°$, we cannot eliminate the shoulders in Figures 21 and 26. However, this is not a serious limitation, especially in view of the fact that we have been able to scan over ± 10 beamwidths simply by switching the source excited.

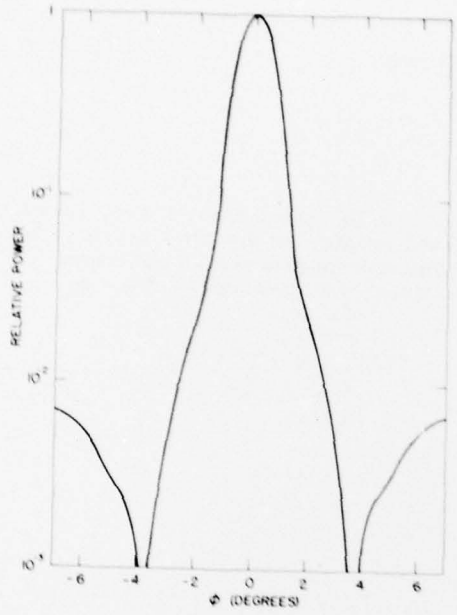

Figure 21. Radiation Pattern Produced When a Line Source is Located at $x/r_o = 0$, $z/r_o = 0.277$ and Illuminates the Reflector With the Power Pattern $\sin c^2 (3.6\theta)$. Also $r_o = 28.5\lambda$

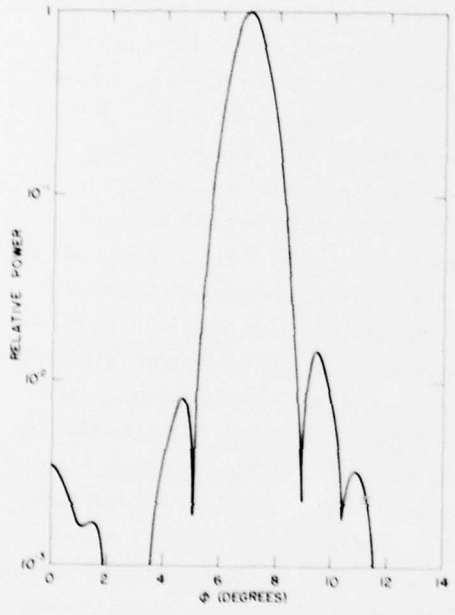

Figure 22. Radiation Pattern Produced When a Line Source is Located at $x/r_o = -0.095$, $z/r_o = 0.25$ and Illuminates the Reflector With the Power Pattern $\sin c^2 [3.6 (\theta + 0.33)]$. Also $r_o = 28.5\lambda$

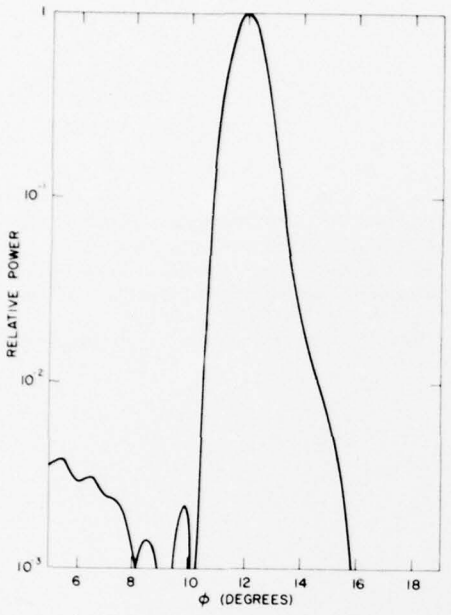

Figure 23. Radiation Pattern Produced When a Line Source is at $x/r_o = -0.154$, $z/r_o = 0.2$ and Illuminates the Reflector With the Power Pattern sinc^2 $[3.6\,(\theta + 0.7)]$. Also $r_o = 28.5\lambda$

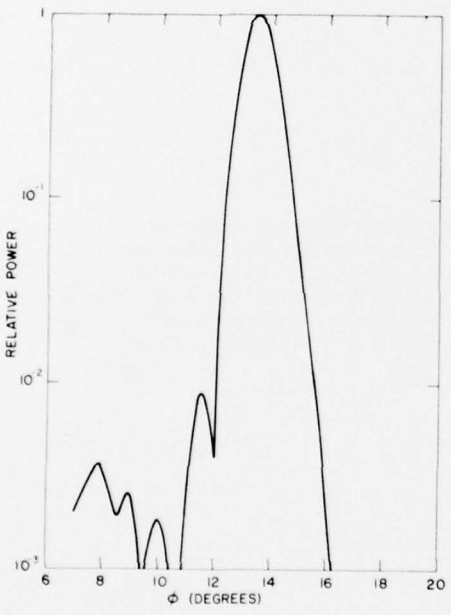

Figure 24. Radiation Pattern Produced When a Line Source is at $x/r_o = 0.17$, $x/r_o = 0.18$ and Illuminates the Reflector With Power Pattern sinc^2 $[3.6\,(\theta + \pi/4)]$. Also, $r_o = 28.5\lambda$

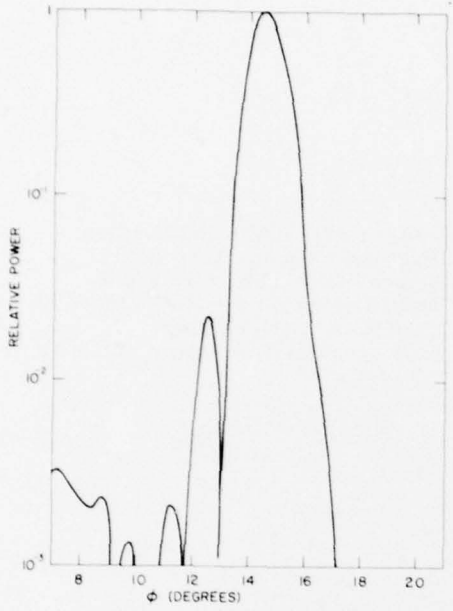

Figure 25. Radiation Pattern Produced When a Line Source is Located at $x/r_o = 0.175$, $z/r_o = 0.16$ and Illuminates the Reflector With the Power Pattern $\text{sinc}^2 [3.6\ (\theta + \pi/4)]$. Also $r_o = 28.5\lambda$

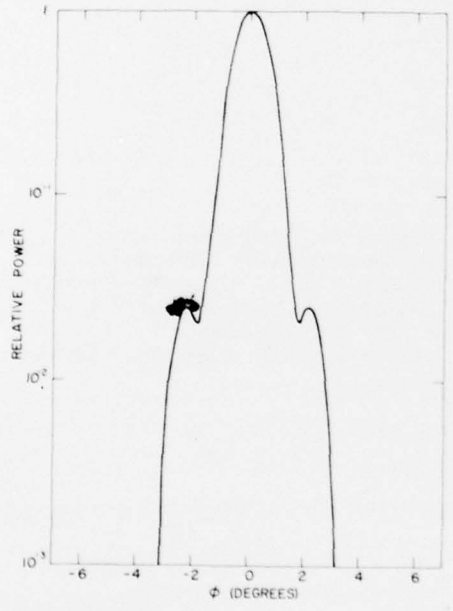

Figure 26. Radiation Pattern Produced When a Line Source is Located at $x/r_o = 0$, $z/r_o = 0.277$ and Illuminates the Reflector With the Power Pattern $\text{sinc}^4 (2.72\ \theta)$. Also $r_o = 28.5\lambda$

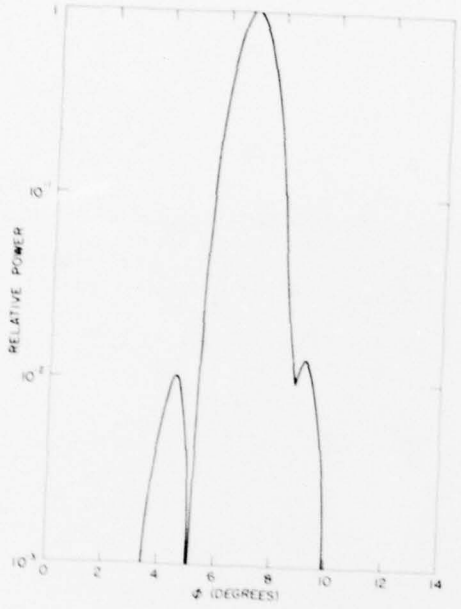

Figure 27. Radiation Pattern Produced When a Line Source is Located at $x/r_o = -0.095$, $z/r_o = 0.25$ and Illuminates the Reflector With the Power Pattern $\sin^4 [2.72 (\theta + 0.33)]$. Also $r_o = 28.5\lambda$

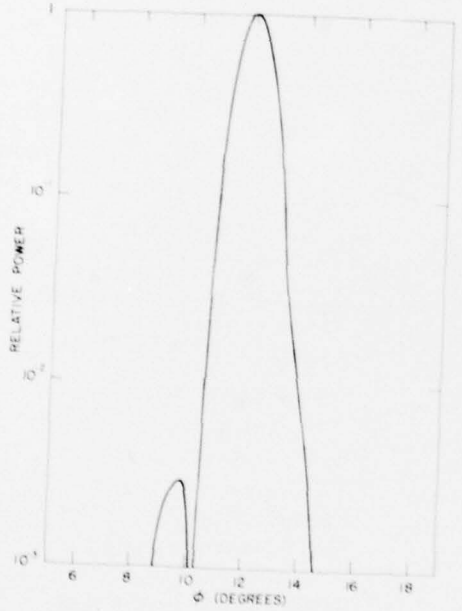

Figure 28. Radiation Pattern Produced When a Line Source is Located at $x/r_o = -0.154$, $z/r_o = 0.2$ and Illuminates the Reflector With the Power Pattern $\sin^4 [2.72 (\theta + 0.7)]$. Also $r_o = 28.5\lambda$

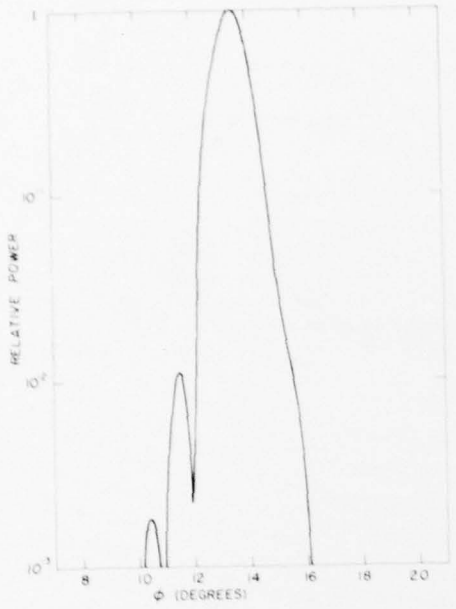

Figure 29. Radiation Pattern Produced When a Line Source is Located at $x/r_o = -0.17$, $z/r_o = 0.18$ and Illuminates the Reflector With the Power Pattern $\sin c^4 [2.72 (\theta + \pi/4)]$. Also, $r_o = 28.5\lambda$

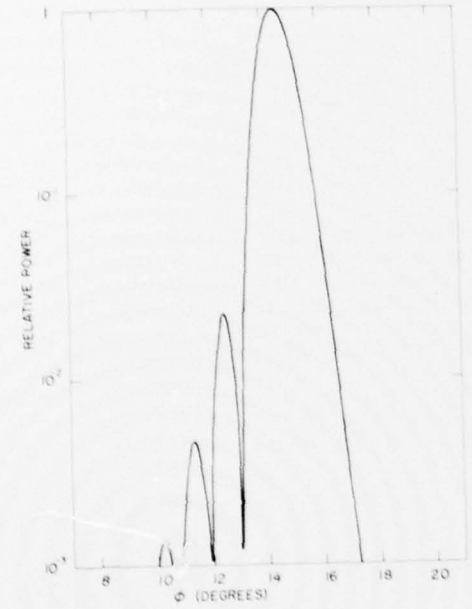

Figure 30. Radiation Pattern Produced When a Line Source Located at $x/r_o = -0.175$, $z/r_o = 0.16$ and Illuminates the Reflector With the Power Pattern $\sin c^4 [2.72 (\theta + \pi/4)]$. Also $r_o = 28.5\lambda$

3. DISCUSSION

Although the reflector discussed has some very attractive features, it also has some serious drawbacks. Primary among these is the fact that the system inherently has a low efficiency because only a portion of the aperture is used in forming any given beam. Calculations of efficiency have given numbers between 25 and 44 percent, depending on the illumination. This latter number corresponds to an illumination function which is constant from $-40° \leq \theta \leq 40°$ and drops rapidly to zero for $|\theta| > 40°$. Realistic aperture illumination functions, however, give efficiencies of 25 to 30 percent.

Another disadvantage of the singly curved reflector considered is that there is considerable blockage of the reflector by the line-source feeds. This can be eliminated by using doubly curved surfaces (so that the feed is a single horn rather than a line source) or by going to offset singly-curved surfaces. In the next phase of this study we will consider the scanning patterns of doubly curved reflectors which have a central profile given by Eq. (2). We will also consider the scanning patterns of appropriate single curved reflectors in which the line source feeds are offset so that there is no blockage of the reflector.

MISSION
of
Rome Air Development Center

RADC plans and executes research, development, test and selected acquisition programs in support of Command, Control Communications and Intelligence (C^3I) activities. Technical and engineering support within areas of technical competence is provided to ESD Program Offices (POs) and other ESD elements. The principal technical mission areas are communications, electromagnetic guidance and control, surveillance of ground and aerospace objects, intelligence data collection and handling, information system technology, ionospheric propagation, solid state sciences, microwave physics and electronic reliability, maintainability and compatibility.

Printed by
United States Air Force
Hanscom AFB, Mass. 01731